2010 IEEE International Conference on Robotics and Automation
Anchorage Convention District
May 3-8, 2010, Anchorage, Alaska, USA

3-DOF Cartesian Force Limiting Device Based on the Delta Architecture for Safe Physical Human-Robot Interaction

Nicolas Lauzier and Clément Gosselin

Abstract— **This paper presents a device that significantly improves the safety of ceiling-mounted robots whose end effector orientation remains constant with respect to the vertical direction (e.g. Scara-type robots). The device consists of a three-degree-of-freedom (DOF) parallel mechanism with the Delta architecture on which the revolute actuators have been replaced with torque limiters. The resulting Cartesian force limiting device (CFLD) is implemented as a mechanical connection between the robot and the effector. It is rigid unless excessive forces are applied on the end effector, for example during a collision. The magnitude of force that activates the mechanism is set by properly adjusting the threshold of the torque limiters. Furthermore, a collision can be rapidly detected with a limit switch placed on one of the links of the mechanism and a signal can be sent directly to brakes that will stop the robot, without passing through a controller and thus improving the reliability and reaction-time of the safety system. By mechanically disconnecting the robot from its end effector, the device ensures that the person involved in the collision is only subjected to the inertia of the end effector and thus potential injuries are greatly reduced. This work is the extension of a previous 2-DOF CFLD that was sensitive only to horizontal forces. The new architecture reacts to collisions occuring in any direction and is geometrically optimized for the proposed application. Also, means to achieve gravitity compensation are proposed.**

I. INTRODUCTION

Integrating robots in the workspace or living space of humans is a goal that is currently pursued by many roboticists and researchers. Physical human-robot interaction (pHRI) would be beneficial in many ways, particularly when considering the possibility to combine the force and endurance of the machine with the judgment and adaptability of the human. Even with promises such as productivity gains in factories, reductions of work-related injuries and improvements of the autonomy for elderly people, this integration is constrained by safety requirements. Indeed, safety should always be the first priority in the design of human interaction robots.

To build safe robots, engineers and researchers are using three different strategies:

1) to develop algorithms that use vision systems or proximity sensors to *anticipate* and *avoid* potentially harmful contacts (see for instance [1], [2]);
2) to *detect* a collision by monitoring joint torques or a robot skin and quickly *react* to maintain the contact forces under a certain level (see for instance [3], [4]);
3) to *design* robots that are *intrinsically safe*, *i.e.*, that are physically unable to hurt a person (see for instance [5], [6], [7], [8], [9], [10], [11], [12], [13]).

It is clear that the *avoidance*, *reaction* and *design* strategies can be combined together to create safer and more dependable robots. However, the first two options alone cannot fully guarantee human safety. This can be explained by considering that a robot intended to interact physically with a person will require the ability to distinguish desirable and undesirable contacts (or *good* and *bad* contacts). This can be done either by disabling safety sensors on the robot parts intended to interact or by running an algorithm that will decide if the upcoming contacts are desirable or not. In either case, safety is compromised either by unprotecting certain parts of the manipulator or by giving the robot some sort of 'judgment capability' which, even in the case of the human, is condemned to occasionally be wrong. Furthermore, the *avoidance* and *reaction* strategies rely on electronic components that can fail. Finally, one could argue that an operator would feel unsecure working with a powerful machine with his safety guaranteed only by an algorithm. It can thus be concluded that the only way to obtain *safe* and *dependable* robots is to use the *design* strategy, which leads to the development of robots that are *intrinsically safe*.

A popular approach to create *intrinsically safe* robots is to make them compliant. Indeed, compliance reduces the peak force attained during a collision. By extending the duration of the contact, it also allows the controller to sense it and react to reduce potential damages, under certain constraints (*i.e.*, reaction time). However, adding compliance limits the precision and stiffness of the robot. Thus, a compromise must be achieved between safety and performance. Also, as explained in [8], compliant joints can store potential energy that allows them to reach higher velocities than their actuators. It can be argued that storing and releasing energy without good controllability can result in unsafe behaviour.

A more recent approach [11], [12], [13], referred to here as force limiting devices, consists in using torque limiters to create stiff robots that become compliant after a contact force threshold is reached. As it can be seen in Fig. 1, force limiting devices allow high stiffness and precision for low interaction forces (in normal conditions) and high compliance and safety when the interaction forces exceed a preset threshold, for example during a collision. This approach thus circumvents the need of a compromise between precision and safety. A video accompanying this paper presents an experimental comparison of collisions using a stiff coupling,

This work was supported by the Natural Sciences and Engineering Research Council of Canada (NSERC) as well as by the Canada Research Chair Program and General Motors (GM) of Canada.

The authors are with the Department of Mechanical Engineering, Université Laval, Québec, Québec, Canada, G1V 0A6, nicolas.lauzier.1@ulaval.ca, gosselin@gmc.ulaval.ca

978-1-4244-5040-4/10/$26.00 ©2010 IEEE

a compliant coupling or a torque limiter on the last actuator of a 4-DOF serial arm.

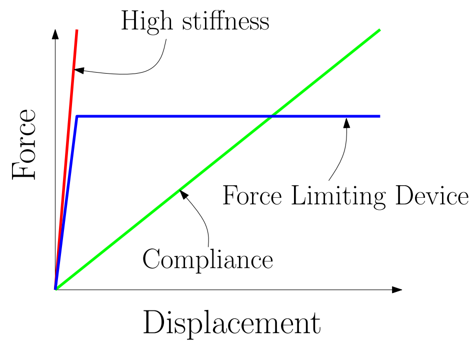

Fig. 1. Contact force as a function of displacement for various stiffnesses.

In [13], a Cartesian Force Limiting Device (CFLD) that can be installed between a suspended robot and its end effector is presented. The device consists of a 2-DOF parallel mechanism with a parallepipedic architecture that constrains the orientation and allow only pure translation of the end effector. Two revolute joints on the mechanism are replaced with torque limiters and thus under normal conditions the end effector is fixed rigidly to the robot. However, if a collision occurs, the torques passing through the limiters become too high and the mechanism is allowed to move. This practically "disconnects" the end effector from the robot and thus the person involved in the collision is only subjected to the inertia of the end effector, which can be significantly lower than the inertia of the whole robot. For the mechanism to be effective at improving safety, the collision has to be detected and the robot must stop before the mechanism reaches the end of its travel. The collision can be detected with a limit switch placed on one of the links and an emergency stop signal can be sent directly to brakes without passing through the controller, thus improving the reliability of the system by reducing the risks of electronic components failure. One important advantage of the parallepipedic architecture is that the torque passing through the limiter only depends on the magnitude of the horizontal force applied on the end effector and is not affected by the location of the point of application of the force. The threshold is however dependant on the force vector orientation and since the optimal achievable forces space is a square, the ratio between the minimum and maximum threshold is $\frac{\sqrt{2}}{2}$ ($\approx 71\%$). The concept has been validated experimentally with a small scale prototype.

In this paper, a 3-DOF CFLD using the Delta architecture which is sensitive to collisions occuring in any direction is presented. This is an important improvement over the 2-DOF mechanism that was only sensitive to horizontal collisions. The architecture itself is first presented before being geometrically optimized for its CFLD application. After, means to achieve gravity compensation are discussed.

II. PRESENTATION OF THE ARCHITECTURE

Fig. 2 shows a 3-DOF CFLD with the Delta architecture and its main design parameters while Fig. 3 illustrates the behaviour of such a mechanism during a collision with a person. An animation accompanying this paper also shows a collision using this type of CLFD. This architecture comprises 3 legs, each composed of a torque limiter that positions the upper link of a parallelogram whose lower link is the lower platform. Each joint of the parallelogram is schematically represented by a spherical joint, although it is usually more practical to use universal joints (spherical joints leave unconstrained the rotation of the side links of the parallelograms along their axes). The parallelograms constrain the orientation of the lower platform such that the two platforms always have the same orientation relative to each other. The mechanism, when activated by forces above the preset threshold, can perform translation in the x, y and z directions.

For the application discussed in this report, it is assumed for symmetry reasons that the optimal design of a CFLD using the Delta architecture will comprise identical legs that are equally spaced, i.e., placed at $120°$ relative to one another with equal radii for attachment points on the platforms. With these simplifications in mind and using the same notation as in [14], the design parameters are:

- r_a: offset of the torque limiter's axis relative to the geometric centre O_a of the upper platform;
- r_b: offset of the parallelogram's attachment point relative to the geometrical centre O_b of the lower platform;
- L_1: length of the side members of the parallelograms;
- L_2: length of the upper members of the legs.

It is important to note that the width of the parallelograms does not affect the kinematics and is thus not considered in this section. However, this dimension affects the structural resistance of the mechanism when subjected to moments applied on the end effector and thus it is of great importance in the design of CFLDs using this architecture.

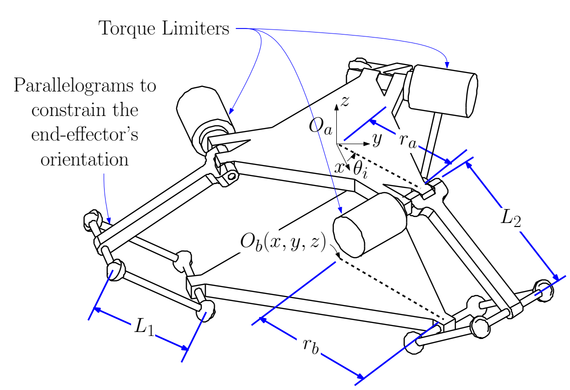

Fig. 2. Cartesian force limiting device with Delta architecture.

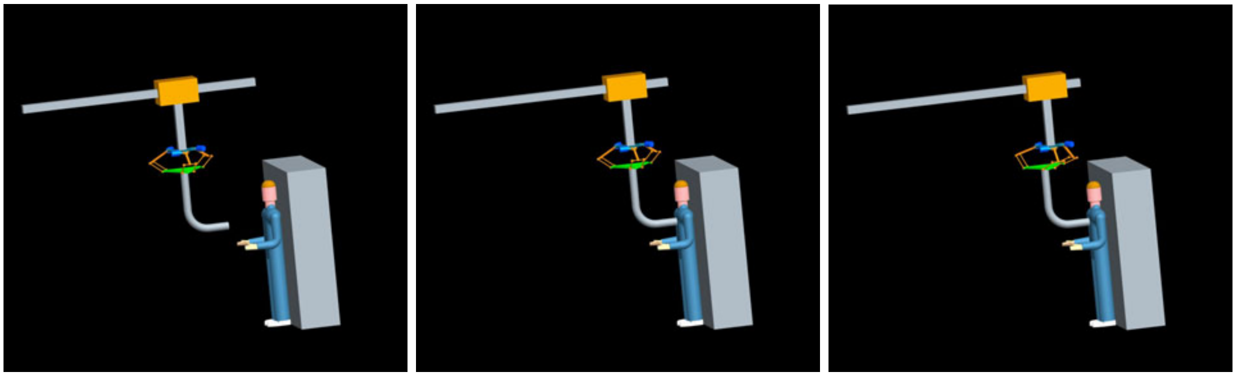

(a) Before collision (b) Collision (c) After collision

Fig. 3. Collision between a person and a ceiling-mounted robot with a 3-DOF CFLD with Delta architecture. These frames are part of an animation accompanying this article.

III. GEOMETRIC OPTIMIZATION OF THE ARCHITECTURE

Two kinematic properties of the mechanism need to be optimized to obtain an effective CFLD. The first one is the workspace of the mechanism. Since the robot must be capable of braking without reaching the CFLD's motion limit, the optimal workspace will be a sphere centred at its reference point (where all torque limiters are in their *locked* angular positions). The radius of that sphere needs to be equal to the maximum braking distance of the robot if we consider collisions occuring in any direction.

Since the threshold depends on the orientation of the external force vector, the second property is the isotropy of the Jacobian matrix of the mechanism. As it was explained in [13], an isotropic Jacobian matrix will maximize the ratio of the minimum over the maximum forces needed to activate the CFLD. For a 3-DOF device, the optimal achievable force polyhedron is a cube and the corresponding ratio between the maximum and minimum activation forces is $\frac{\sqrt{3}}{3}$ ($\approx 58\%$).

To simplify the optimization, it is possible to express each dimension of the mechanism as a ratio to the length of the first member of each leg L_2. This simplification is allowed by the fact that the two properties can be optimized regardless of the scale of the mechanism. Isotropy depends only on the dimensions' ratios, whereas the radius of the spherical workspace can be maximized as a ratio of L_2. Afterwards, the mechanism can be scaled by adjusting the value of L_2 to match the size of the workspace with the application's requirements.

As shown in Fig. 4, the following dimensionless parameters are used to optimize the architecture:

- $\eta = \frac{-z_0}{L_2}$ represents the relative height of the vertical position of the neutral configuration of the device, where all the torque limiters are fixed. This is the only configuration of the mechanism in normal conditions.
- $\alpha = \frac{r_a - r_b}{L_2}$ is the relative offset of the attachment points of the leg to the upper and lower platforms. It is important to note that, kinematically, only the difference and not the actual values of r_a and r_b affects the workspace and the isotropy of the mechanism.

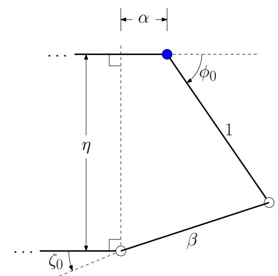

Fig. 4. Schematic representation of one of the legs in its reference position and in the plane normal to its torque limiter. All the lengths are normalized relative to the first member's length.

- $\beta = \frac{L_1}{L_2}$ is the ratio between the lengths of the two leg members.
- ϕ_0 is the angle of the upper bar relative to the horizontal.
- ζ_0 is the angle of the lower bar relative to the horizontal.

It should be noted that ϕ_0 and ζ_0 are not independent from η, β and α and thus they are not independent design parameters but rather dependent variables that simplify the optimization. Hence, there are three design parameters for two properties to optimize. This means that a degree of freedom will be left in the design of the device. This remaining variable will be used to add flexibility in the mechanical design of the device, for example to avoid geometric interference between the parts.

a) Maximal Spherical Workspace Constraint: for parallel mechanisms, the workspace is always equal to the intersection of all the legs' sub-workspaces. In this case, each of these workspaces is a torus centred on the leg's upper attachment point with a major radius of 1, a minor radius of β and the revolution axis being the one of the upper pivot (the torque limiter's axis). Because the torus is formed by the revolution of a circle (or a sphere) of radius β, the largest sphere that can be inserted in the torus will also have a radius of β. Therefore, the maximal spherical workspace of the mechanism will have a radius of β and will be centred at $(0, 0, -\eta)$ if, and only if, the revolution paths of all the legs' toruses intersect at this point. This constraint, represented on Fig. 5, can be expressed by the following equation:

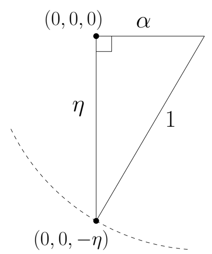

Fig. 5. Schematic representation of the maximum volume constraint.

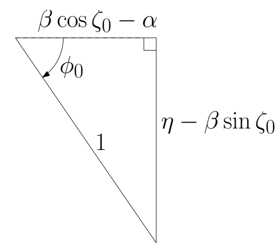

Fig. 6. Schematic representation of the upper triangle of the leg in its reference position.

$$\eta = \sqrt{1-\alpha^2}. \tag{1}$$

b) Jacobian Matrix Isotropy Constraint: a matrix is isotropic when it is a multiple of an orthogonal matrix. To derive the constraint, the first step is to obtain an expression for the Jacobian matrix. The kinematic constraint for each leg is [14] :

$$g_j = (x_j - x_p)^2 + (y_j - y_p)^2 + (z_j - z_p)^2 - {L_1}^2 = 0 \tag{2}$$

where (x_p, y_p, z_p) are the coordinates of the platform reference point and (x_j, y_j, z_j) are the coordinates of the connection point between the members L_1 and L_2 of the j^{th} leg, i.e.:

$$x_j = (r + L_2 \cos\phi_{1j})\cos\theta_j, \tag{3}$$
$$y_j = (r + L_2 \cos\phi_{1j})\sin\theta_j, \tag{4}$$
$$z_j = -L_2 \sin\phi_{1j}. \tag{5}$$

In these equations, $r = r_A - r_B$ is the offset between the upper and lower attachment points on the platforms, ϕ_{1j} and θ_j are the angle of the first member of the j^{th} leg relative to the horizontal and the x-z plane, respectively.

It is possible to differentiate eq. (2) with respect to time to obtain the Jacobian matrices of the mechanism as:

$$\mathbf{J}' \begin{bmatrix} \dot\phi_{11} \\ \dot\phi_{12} \\ \dot\phi_{13} \end{bmatrix} = \mathbf{K}' \begin{bmatrix} \dot x_p \\ \dot y_p \\ \dot z_p \end{bmatrix} \tag{6}$$

which can also be written as:

$$\begin{bmatrix} \dot\phi_{11} \\ \dot\phi_{12} \\ \dot\phi_{13} \end{bmatrix} = (\mathbf{J}')^{-1}\mathbf{K}' \begin{bmatrix} \dot x_p \\ \dot y_p \\ \dot z_p \end{bmatrix} = \mathbf{K} \begin{bmatrix} \dot x_p \\ \dot y_p \\ \dot z_p \end{bmatrix} \tag{7}$$

From the kinematic-static duality, the problem consists in making isotropic the transpose of matrix $\mathbf{K}$, that is:

$$\mathbf{K}^T = [(\mathbf{J}')^{-1}\mathbf{K}']^T = (\mathbf{K}')^T(\mathbf{J}')^{-T} \tag{8}$$

It can however be observed that matrix $(\mathbf{J}')^{-T}$ is diagonal because g_j only depends on ϕ_{1j}. Also, because of the symmetry of the mechanism in its neutral configuration, all the diagonal entries are the same and thus $(\mathbf{J}')^{-T}$ is isotropic. Therefore, the condition will be achieved if $(\mathbf{K}')^T$ is also isotropic. This is the case if the columns of $(\mathbf{K}')^T$ all have the same magnitude (which is verified because of the symmetry between the legs in the neutral configuration) and if their inner products are zero, namely:

$$\mathbf{k}_i^T\mathbf{k}_j = 0, \quad \forall i \neq j, \quad (\mathbf{K}')^T = \begin{bmatrix} \mathbf{k}_1 & \mathbf{k}_2 & \mathbf{k}_3 \end{bmatrix}. \tag{9}$$

The following simplifications, based on the symmetry of the mechanism and on the fact that the neutral position is centred on the z axis, are obtained:

$$x_p = 0, \quad y_p = 0, \quad \phi_{11} = \phi_{12} = \phi_{13} = \phi_0. \tag{10}$$

Hence, by using the ratios of the lengths relative to L_2 defined above, we obtain, after some manipulations and trigonometric transformations, the following expression for $\mathbf{k}_i^T\mathbf{k}_j$:

$$\mathbf{k}_i^T\mathbf{k}_j = \left(\alpha^2 + 2\,\alpha\,\cos\phi_0 + \cos^2\phi_0\right)\cos(\theta_i - \theta_j) + 1 - \cos^2\phi_0 - 2\,\eta\sin\phi_0 + \eta^2 = 0. \tag{11}$$

However, because the three legs are symetrically separated by 120 degrees, it can be seen that:

$$\cos(\theta_i - \theta_j) = \cos\left(\pm\frac{2\pi}{3}\right) = -\frac{1}{2}, \quad \forall i \neq j. \tag{12}$$

Also, from Fig. 6, that represents the upper triangle of the leg shown in Fig. 4, the following substitutions can be made:

$$\cos\phi_0 = \beta\cos\zeta_0 - \alpha, \tag{13}$$
$$\sin\phi_0 = \eta - \beta\sin\zeta_0, \tag{14}$$

which leads to, after some manipulations:

$$4\,\beta^2\left(1 - 3/2\,\cos^2\zeta_0\right) = 0. \tag{15}$$

Finally, the latter expression is solved for ζ_0:

$$\zeta_0 = \left\{\cos^{-1}\left(\sqrt{\frac{2}{3}}\right), \quad \pi - \cos^{-1}\left(\sqrt{\frac{2}{3}}\right)\right\}. \tag{16}$$

The second solution corresponds to the leg oriented to the interior of the mechanism, which is not desirable because of possible mechanical interferences. Thus, $\zeta_0 = \cos^{-1}\left(\sqrt{\frac{2}{3}}\right)$ is chosen, which gives $\cos\zeta_0 = \sqrt{\frac{2}{3}}$ and $\sin\zeta_0 = \sqrt{\frac{1}{3}}$, leading to:

$$1 = \cos^2\phi_1 + \sin^2\phi_1 = \beta^2 - \frac{2\sqrt{6}}{3}\beta\,\alpha + \alpha^2 + \eta^2 - \frac{2\sqrt{3}}{3}\eta\,\beta. \quad (17)$$

Using eq. (1) for the value of η and solving for α as a function of β, we obtain two solutions for α. However, only the smallest is physically possible since for $0 < \beta \leq 1$, the largest root will give $\alpha > 1$, which is incompatible with the maximum volume constraint given by eq. (1). Selecting the smallest root:

$$\alpha = \frac{\sqrt{6}}{6}\beta - \frac{\sqrt{3}}{3}\sqrt{1 - \frac{\beta^2}{4}} \quad (18)$$

guarantees the isotropy of the mechanism in its neutral configuration, while being compatible with the maximum volume constraint. These constraints thus link the dimensionless parameters α and η as functions of β to get an optimal design in the sense of the chosen objectives. The remaining variable β, is chosen to maximize the workspace without allowing geometric interferences between the parts of the mechanism. Fig. 7 shows the effect of β on the maximum spherical workspace.

IV. GRAVITY BALANCING

As mentioned above, the 3-DOF device proposed here is sensitive to vertical forces, which is a desired property since collisions can occur in any direction. However, this property introduces a new challenge in the sense that the weight of the end effector induces torques at the limiters. For large payloads, the torques can be close to or higher than the limits set for safety requirements, thus compromising the effectiveness of the device to improve safety while maintaining performances. For this reason, gravity balancing is necessary when the combined weight of the payload and the end effector is large relative to the force limit imposed by the device.

There is an available balancing method that takes advantage of the fact that the CFLD mechanism needs to be balanced in only one configuration. Indeed, balancing a parallel mechanism is usually complex because of the nonlinear and coupled relations between Cartesian and articular displacements. However, CFLDs are a special class of mechanism in the sense that they are intended to work in a single configuration, except when collisions occur. In this case, having the mechanism balanced is not important since a collision corresponds to an emergency situation in which the robot's performances are not a concern. Therefore, it is acceptable to have a mechanism that balances the weight of the end effector only in the neutral configuration. This mechanism can be as simple as a pre-loaded spring, as shown in Fig. 8. This method is valid only if the spring does not limit the workspace of the device, which might only be possible for smaller leg length ratios β (see section III).

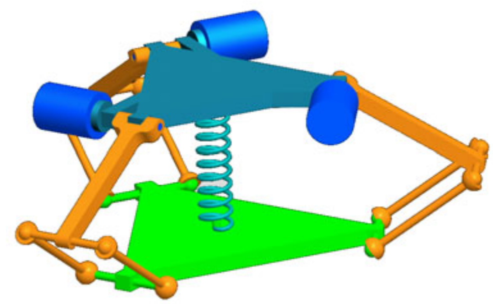

Fig. 8. Force limiting device balanced with a loaded spring.

Springs have the advantage of adding little weight and complexity to the system if the payload is constant. However, balancing variable loads with a spring requires an actuator to modify the position of one of its anchor points. This is inconvenient since the actuator must provide a force equal to the payload itself. However, it is possible to envision a system in which the same actuator would move the end effector in normal mode and adjust the CFLD's balancing force when the robot is picking up a new load. To do so, the spring's upper anchor point could be mounted on a linear guide with a locking system. An example of such mechanism is presented in Fig. 9. In normal mode, the anchor point is locked and thus the actuator is displacing M_1, and then M_2 via the CFLD. However, when the robot is picking up or releasing a part, the anchor point is unlocked and thus the actuator is displacing M_2 via the spring, and then M_1 via the CFLD. If for example the new load is heavier, it will thus pull on the spring until the elastic force in the spring reaches a force equal to M_2's weight. Then, the anchor point is locked again and the system goes back to normal mode where the whole end effector (M_1 and M_2) can be displaced vertically. However, this strategy requires M_1's weight to be lower than the maximum transmitted force since it is supported by the CFLD during the adjustment phase of the cycle.

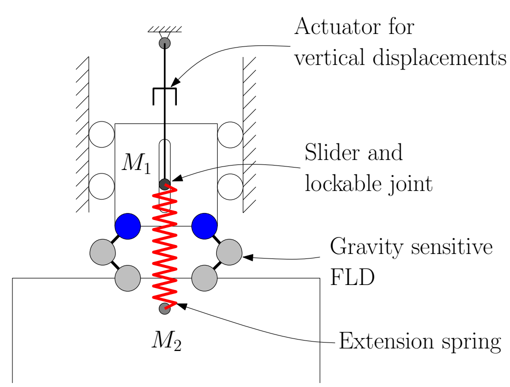

Fig. 9. Mechanism to balance variable loads with a spring.

There is no precise way to determine if, for one particular application, the safety gains from balancing are worth the increased complexity of the system. If the payload is small compared to the force threshold, it is preferable to let the

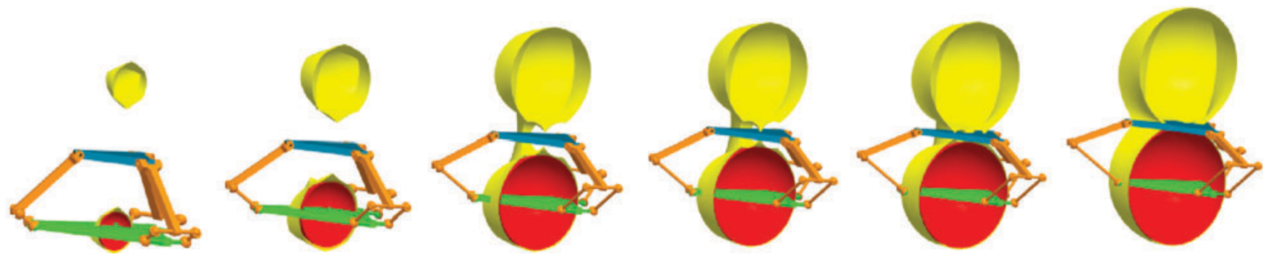

(a) $\beta = 0.25$ (b) $\beta = 0.50$ (c) $\beta = 0.75$ (d) $\beta = 0.80$ (e) $\beta = 0.90$ (f) $\beta = 1.00$

Fig. 7. 3-DOF CFLD with Delta architecture satisfying the maximum volume and isotropy constraints for different leg ratios β. The attainable and spherically optimized workspaces are shown in yellow and red, respectively. The torque limiters are not shown for simplicity.

system unbalanced. For some applications, it might even be preferable to cover only horizontal collisions and thus to use CFLDs that have only 1 or 2 DOFs.

V. CONCLUSIONS AND FUTURE WORK

In this paper, a 3-DOF Cartesian force limiting device has been proposed to improve the safety of ceiling-mounted robots with constant end effector orientation relative to the vertical. The mechanism is based on the Delta architecture in which three revolute joints are replaced by torque limiters. It behaves as a rigid connection between the robot and its end effector. However, if an excessive force is applied during a collision, the mechanism is activated and thus the end effector is free to move relatively to the robot. The activation of the mechanism is detected and brakes are applied to stop the robot. The inertia of the parts located upstream of the device (above) is thus removed from the collision. Also, for a quasi-static collision in which a person is clamped between the robot and a wall, the maximum contact force is the activation force for that orientation, as determined by the configuration of the torque limiters. Hence, the safety is improved for all types of blunt collisions.

This new mechanism is an extension of a 2-DOF mechanism that was presented by the authors in a previous paper [13]. The novel device is preferable since it can protect persons from collisions occuring in any direction on the end effector. The force threshold is also independent from the position of the contact point, which is a significant advantage when the collision can occur anywhere on the end effector. The geometry of the device has been optimized to maximize its workspace and to lead to an isotropic Jacobian matrix in its neutral configuration. Means of compensating gravity were also proposed for applications in which the payload has a weight similar to the force threshold imposed for safety reasons.

Future work includes the experimental confirmation of the safety gains obtained with CFLDs in terms of their effect on various safety indices. The development of articular force limiting devices (or AFLDs), which correspond to the addition of a torque limiter in series with each actuator on a serial robot will also be pursued. The improvements attained by using torque limiters that are adjustable online will be investigated theoretically and experimentally.

REFERENCES

[1] D. Ebert, T. Komuro, A. Namiki, and M. Ishikawa, "Safe human-robot-coexistence: emergency-stop using a high-speed vision-chip," in *IEEE/RSJ International Conference on Intelligent Robots and Systems (IROS 2005)*, 2005, pp. 2923–2928.

[2] Y. Lu, L. Zeng, and G. M. Bone, "Multisensor system for safer human-robot interaction," in *IEEE International Conference on Robotics and Automation (ICRA 2005)*, 2005, pp. 1767–1772. [Online]. Available: http://ieeexplore.ieee.org/xpls/abs_all.jsp?arnumber=1570369

[3] V. Duchaine, N. Lauzier, M. Baril, M.-A. Lacasse, and C. Gosselin, "A flexible robot skin for safe physical human robot interaction," in *IEEE International Conference on Robotics and Automation (ICRA 2009)*, 2009, pp. 3676–3681.

[4] A. De Luca, A. Albu-Schäffer, S. Haddadin, and G. Hirzinger, "Collision detection and safe reaction with the DLR-III lightweight manipulator arm," in *IEEE/RSJ International Conference on Intelligent Robots and Systems (IROS 2006)*, 2006, pp. 1623–1630.

[5] G. Tonietti, R. Schiavi, and A. Bicchi, "Design and control of a variable stiffness actuator for safe and fast physical human/robot interaction," in *IEEE International Conference on Robotics and Automation (ICRA 2005)*, 2005, pp. 526–531. [Online]. Available: http://ieeexplore.ieee.org/xpls/abs_all.jsp?arnumber=1570172

[6] B.-S. Kim, J.-J. Park, and J.-B. Song, "Double actuator unit with planetary gear train for a safe manipulator," in *IEEE International Conference on Robotics and Automation (ICRA 2007)*, 2007, pp. 1146–1151.

[7] J. Choi, S. Park, W. Lee, and S. Kang, "Design of a robot joint with variable stiffness," in *IEEE International Conference on Robotics and Automation (ICRA 2008)*, 2008, pp. 1760–1765.

[8] S. Wolf and G. Hirzinger, "A new variable stiffness design: Matching requirements of the next robot generation," in *IEEE International Conference on Robotics and Automation (ICRA 2008)*, 2008, pp. 1741–1746.

[9] M. Zinn, O. Khatib, and B. Roth, "A new actuation approach for human friendly robot design," in *IEEE International Conference on Robotics and Automation (ICRA 2004)*, 2004, pp. 249–254.

[10] I. Sardellitti, J. Park, D. Shin, and O. Khatib, "Air muscle controller design in the distributed macro-mini (DM2) actuation approach," in *IEEE/RSJ International Conference on Intelligent Robots and Systems (IROS 2007)*, 2007, pp. 1822–1827.

[11] J.-J. Park, J.-B. Song, and H.-S. Kim, "Safe joint mechanism based on passive compliance for collision safety," *Recent Progress in Robotics: Viable Robotic Service to Human*, pp. 49–61, 2008.

[12] J.-J. Park, H.-S. Kim, and J.-B. Song, "Safe robot arm with safe joint mechanism using nonlinear spring system for collision safety," in *IEEE International Conference on Robotics and Automation (ICRA 2009)*, 2009, pp. 3371–3376.

[13] N. Lauzier, M. Grenier, and C. Gosselin, "2 dof cartesian force limiting device for safe physical human-robot interaction," in *IEEE International Conference on Robotics and Automation (ICRA 2009)*, 2009, pp. 253–258.

[14] M. Laribi, L. Romdhane, and S. Zeghloul, "Analysis and dimensional synthesis of the delta robot for a prescribed workspace," *Mechanism and Machine Theory*, vol. 42, no. 7, pp. 859 – 870, 2007.